Proceedings of the 10o Brazilian Congress of Thermal Sciences and Engineering -- ENCIT 2004
Braz. Soc. of Mechanical Sciences and Engineering -- ABCM, Rio de Janeiro, Brazil, Nov. 29 -- Dec. 03, 2004

ON-LINE IDENTIFICATION OF HORIZONTAL TWO-PHASE FLOW REGIMES THROUGH GABOR TRANSFORM AND NEURAL NETWORK PROCESSING

Selli, M.F.
Smar Equipamentos Ind. Ltda.
Rua Dr. Antonio Furlan Jr., 1028
Sertãozinho - SP 14170-480
Brazil
mselli@smar.com.br

Seleghim, Jr. P.
NETeF – EESC - USP
Av. Trabalhador Sancarlense, 400
13566-590 São Carlos – SP
Brazil
Seleghim@sc.usp.br

Abstract. *The fundamental objective of this work is the construction of a specialist system capable of diagnosing different configurations of horizontal two-phase flow regimes. It is important to emphasize that the development of this know-how is capital to the efficient operation of facilities for manipulation and transportation of multiphase fluids, and represents today one of the most important challenges in petrochemical and thermonuclear industries.The working principle of the proposed system is based on the signals acquired by a rapid response pressure gradient sensor, and on its post processing through Gabor Transform and on a previously trained artificial neural network. The implementation is accomplished in way that the diagnosis operation is performed on-line, from acquisition of the signal to its post-processing. Experimental results were obtained on the experimental circuit at NETeF – Núcleo de Engenharia Térmica e Fluidos of USP – Universidade de São Paulo, at São Carlos, using a horizontal test section, with 12 m length and 30mm internal diameter. Experiments were done with the following air-water flow regimes: stratified smooth, stratified wavy, intermittent, annular and bubbly. Results show that the percentage of correct flow regime diagnosis in steady state conditions is practically of 100%.*

Keywords*: multiphase flow, flow patterns, neural networks, signal analysis*

1. Introduction

Multiphase flow regimes are very common in industrial pipelines. In the petrochemical industry, for instance, the monitoring of oil-gas flows is more and more necessary for a safe operation in exploration and production fields. The unexpected arrival of slugs at the inlet of three-phase separators installed on off-shore production platforms results in severe transients to their control systems and contributes to reduce the operation efficiency of such equipment. The possibility to interfere on such regimes, together with flow regime inference algorithms, can widen the amount of available information for the operators of such industrial processes, increasing security and efficiency. Another interesting example is the development of new transport technologies for ultra-viscous oils, based on creating an annular regime with the oil phase flowing in the center and the water flowing near the walls of the tube – the so-called core annular flow (Bannwart, 2001). The reduction in the pumping power is dramatic but the applicability of such technology under field conditions depends on the development of active control systems capable of identifying when the annular structure of the flow becomes unstable in order to avoid the imminent regime transition.

The development of objective criteria for detecting flow regimes has been the central objective of many researches. The first approaches were based on the analysis of pressure signals and the corresponding spectra (Hubbard and Dukler, 1966) because such signals are very common in industrial processes. A comprehensive review can be found in Drahos and Cermak (1989). Less restrictive signal analysis techniques, such as adaptative filtering, wavelets and fractals, constituted strong tendencies in the 90's. Interesting methods were proposed for the characterization of flow regimes from fractal or chaotic aspects of the analyzed signal. Also, Hervieu and Leducq (1991) demonstrated the applicability of the wavelet transform in the investigation of vertical gas-liquid flows. In the sequence of this work, Seleghim and Hervieu (1994) proposed an objective indicator for the bubbly-slug transition in vertical flows, based on quantifying the loss of stationarity through the standard deviation of Ville's instantaneous frequency calculated from void signals. This same approach was adopted and improved in the work of Hervieu and Seleghim (1998), in which the time-frequency covariance calculated from the Gabor transform of void signals was acknowledged as a universal flow regime transition indicator. This claim was confirmed in a subsequent work by Klein et al. (2004) which investigated the existence of sub-regimes in intermittent gas-liquid horizontal flow.

A different and also promising approach is the application of connectionist or neural models to the problem of flow regime identification. Among many interesting mathematical properties these models possess the so-called associative memory from which it is possible to infer a correct conclusion from incomplete or truncated input data. One of the first works reported in the scientific literature is probably the article by Mi *et al.* (1998) in which statistical moments calculated from impedance signals were used to classify vertical flow regimes with a supervised neural network. Another prospective work was reported by Crivelaro *et al.* (2002) in which the impedance signals obtained from a direct imaging probe were processed through an elaborated neural architecture constituted of six independent modules, trained to detect specific flow regimes, followed by a winner-take-all layer to resolve conflicts between modules. In a more recent work by Yan *et al.* (2004) trained a classificatory network constituted of multiple exits, one for each flow regime, using simulated data from a capacitive tomographic sensor. In general the results reported in these works are very good, in some cases the probability of correct regime detection nears 100%, but they are all based on impedance signals what is frequently difficult to obtain in field conditions. For instance the piping section on which the sensor is to be installed must be made of a dielectric material. A more applicable approach should be based on the signals obtained from more practical sensors, such as pressure or acceleration transducers. The problem though is that the information regarding the flow structure is not as well structured as it is in impedance signals. On the contrary, it is well known that pressure signals reflect not only the local flow conditions but also many diameters up and downstream the region where it is installed. Acceleration signals have a somewhat similar problem, namely its poor localization, with the additional difficulty of being strongly dependent on the mechanical behavior of the piping (vibration modes, damping, etc.). An adequate method to handle these types of signals (excessively rich) is the time-frequency decomposition: the information contained in the original one-dimensional signal is spread over a 2D distribution and is, therefore, better resolved.

There are many possible time-frequency decompositions such as the Wigner-Ville and Choi-Williams distributions. Also, the wavelet transform can be seen as a time-frequency distribution if the analyzing wavelet has good time and frequency localization properties (strictly speaking it constitutes a time-scale decomposition). We will adopt the Gabor transform in this work because its Gaussian analyzing function equals the minimum of the uncertainty principle (best simultaneously localized in time and frequency), and also for being well suited for on-line processing. The approach adopted in this work is then to use pressure signals, given that they are interesting for industrial applications, to Gabor transform them in order to resolve the useful information and to process the corresponding time-frequency coefficients through a previously trained neural network model in order to detect the flow regime. Our basic assumption is that each flow regime has a characteristic time-frequency signature that can be identified by the neural network. This assumption has been shown to be true by Seleghim et al. (1998) in horizontal gas-liquid flows for impedance signals but, to our knowledge, still remains to be demonstrated for pressure signals. Our main objective is to develop an expert system suited for industrial application and capable of on-line detecting the flow regime in horizontal gas-liquid flow.

The text is organized as follows: introduction of the basic concepts regarding the Gabor transform and neural network models, description of the experimental loop and the corresponding instrumentation used to validate the proposed methodology, information about the experimental tests and results, conclusions and suggestions for future work.

2. The Gabor transform

The analysis of the spectral content based only on Fourier transform may not be sufficient to describe the process or physical phenomena from which the analyzed signal was extracted, mainly because all temporal information is hidden due to the integration on time. In other words, the Fourier transform emphasizes all information regarding frequencies (which frequencies are present) at the cost of temporal aspects (when these frequencies occurred). But in many processes frequencies vary along time and this information, i.e. the modulation law of the spectral content, is usually of utmost importance for the correct interpretation of the signal. Good examples are the so-called tonal languages, such as Mandarin Chinese and Cantonese, in which changes in the pitch of a sound mean completely different words. Thus, the objective of time-frequency analysis is to construct, from the original one-dimensional signal, an associated two-dimensional distribution that identifies the instantaneous or local spectral content, just like in a musical score. There are many possible alternatives for constructing such joint time-frequency distribution. If one recognizes the scalar product as a measure of the similarity between a generic signal $s(\cdot)$ and an analyzing function $h_{t,\omega}(\cdot)$ well localized around the time t and the frequency ω, this joint distribution can be defined as

$$P(t,\omega) = \langle s, h_{t,\omega} \rangle = \int_{-\infty}^{+\infty} s(\tau) h^{*}_{t,\omega}(\tau) d\tau \tag{1}$$

Different definitions for generating the family of analyzing functions lead to different classes of distributions. For instance, if $h_{t,\omega}(\cdot)$ is generated from affine transformations applied to an admissible mother function $h(\cdot)$, that is

$$h_{t,\omega}(\tau) = h\left(\frac{\tau - t}{\omega_o/\omega}\right) \tag{2}$$

than $P(t,\omega)$ becomes the well known wavelet transform which is an example of the affine class. The short time Fourier transform belongs to Cohen's class and is obtained by translating in time and frequency the admissible mother function according to

$$h_{t,\omega}(\tau) = h(\tau - t)e^{i\omega\tau} \tag{3}$$

where $i = \sqrt{-1}$. The Gabor transform corresponds to a special case of a short time Fourier transform in which the mother function is a Gaussian window. That is

$$h(\tau) = e^{-\alpha\tau^2} \tag{4}$$

where α is a parameter controlling the Gaussian's decaying speed. By applying the definition (1) one obtains

$$P(t,\omega) = \int_{-\infty}^{+\infty} s(\tau)e^{-\alpha(\tau-t)^2 - i\omega\tau}d\tau \tag{5}$$

The Gabor transform is an interesting choice because its analyzing function, i.e. translated versions of a Gaussian window, satisfies the minimum of the uncertainty principle. More precisely, by defining a measure of the support of $h(\cdot)$ and of its Fourier transform $h(\cdot)$ according to

$$\Delta_h = \frac{1}{E}\int_{-\infty}^{+\infty}(\tau - t_0)^2\left|h(\tau)\right|^2 d\tau \tag{6}$$

$$\Delta_{\hat{h}} = \frac{1}{E}\int_{-\infty}^{+\infty}(\tau - \omega_0)^2\left|\hat{h}(\tau)\right|^2 d\tau \tag{7}$$

where E stands for the energy of the signal and t_0 and ω_0 respectively for its central time and frequency, then it is possible to demonstrate that

$$\Delta_h \Delta_{\hat{h}} = 2\pi \tag{8}$$

whereas for any other signal $s(\cdot)$, different from a Gaussian window, this relation becomes (Gabor, 1946)

$$\Delta_s \Delta_{\hat{s}} > 2\pi \tag{9}$$

An important consequence of this is that the Gabor transform produces an optimal partition of the time-frequency plane by translating $h(\cdot)$ by steps T in time and Ω in frequency, that is

$$h_{m,k}(\tau) = h(\tau - mT)e^{ik\Omega\tau} \tag{10}$$

where $k = 0, \pm1, \pm2\ldots$ and $m = 0, \pm1, \pm2\ldots$ By defining T and Ω according to

$$T\Omega = \frac{2\pi}{\beta} \tag{11}$$

one obtains a redundant ($\beta > 1$), an exact ($\beta = 1$) or a loose ($\beta < 1$) partition of the time-frequency plane, on which it is possible to associate the following decomposition coefficients (named atoms by Gabor):

$$a_{m,k} = \int_{-\infty}^{+\infty} s(\tau)e^{-\alpha(\tau-mT)^2 - ik\Omega\tau}d\tau \tag{12}$$

In this work these coefficients will be calculated from pressure signals and will be used to identify the flow regime through a previously trained neural network model. For a comprehensive text on time-frequency analysis the reader is pointed to the book by Cohen (1995).

3. Neural network models

A neural network can be defined as a nonlinear mapping of an input onto an output vector space. This is achieved through layers of activation functions or neurons in which the input coordinates are summed according to weighting values and bias to produce single output or firing values. In this work, we used a feed forward network for which there is no recursiveness, i.e. the input vector of a specific neuron layer is formed only by the firing values of the preceding layer, as shown in Fig. (1).

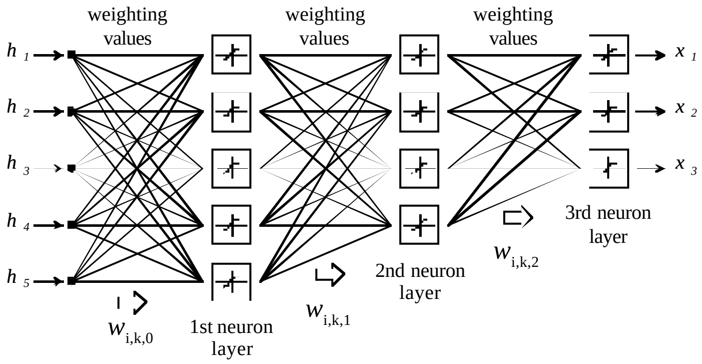

Figure 1. Schematic representation of a feed forward neural network mapping a 5 coordinates input vector onto a 3 coordinates output vector.

Formally, if the activation function of i-th neuron in the j-th layer is indicated by $F_{i,j}(\cdot)$, its output $s_{i,j}$ can be calculated from the outputs of the preceding layer $s_{i,j-1}$ and the corresponding bias $b_{i,j}$ and weighting values $w_{i,k,j-1}$ (the second subscript k indicates the neuron in the (j-1)-th layer from which the connection is being established) according to the expression

$$s_{i,j} = F_{i,j}\left(b_{i,j} + \sum_k w_{i,k,j-1}\, s_{k,j-1} \right) \tag{13}$$

The network's input and output values being denoted respectively by η_i, and ξ_i, the mapping relation of one onto another can be calculated by successively applying (1), what for the example in Fig. (1) results

$$\xi_i = F_{i,3}\left(b_{i,3} + \sum_{k=1}^{4} w_{i,k,2}\, F_{k,2}\left(b_{k,2} + \sum_{m=1}^{5} w_{k,m,1}\, F_{m,1}\left(b_{m,3} + \sum_{n=1}^{5} w_{m,n,0}\, \eta_n \right)\right)\right) \tag{14}$$

Expression (14) makes clear that the relation between η_i, and ξ_i, is unambiguously defined by choosing the activation functions and by setting the bias and weighting values. Among many, a very important characteristic of neural networks is the so-called learning potential, i.e. the possibility of adjusting the bias and weighting values through a convenient training rule to closely reproduce pre-assigned pairs of input/output values. The back-propagation is probably the most used training heuristics and is particularly well adapted to feed forward architectures. It is based on the iterative application of a discrete gradient descent algorithm, computed from the first derivatives of a conveniently defined error function with respect to the parameters of the network. In general lines the basic steps of the back-propagation procedure implemented in this work are the following:

1. Initialize the parameters of the network $b_{i,j}$ and $w_{i,k,j}$ with random numbers
2. From a training data set with pre-assigned input/output pairs take the p-th one (η_i^p, δ_i^p), calculate the outputs of the network with the same input and form the pair (η_i^p, ξ_i^p)
3. Calculate the error between the desired (δ_i^p) and the obtained (ξ_i^p) output values according to the Euclidean norm

$$e = \sqrt{\sum_i (\delta_i^p - \xi_i^p)^2} \tag{15}$$

4. Calculate the derivatives of the error e with respect to $b_{i,j}$ and $w_{i,k,j}$
5. Modify the network parameters according to a steepest descent strategy and a specified learning rate γ

$$b_{i,j} \leftarrow b_{i,j} - \gamma \frac{\partial e}{\partial b_{i,j}} \quad \text{and} \quad w_{i,k,j} \leftarrow w_{i,k,j} - \gamma \frac{\partial e}{\partial w_{i,k,j}} \tag{16}$$

6. Iterate from 2 to 5, successively modifying $b_{i,j}$ and $w_{i,k,j}$, until a defined number of learning epochs (cycles) or a convenient stopping criterion be achieved

The performance of a neural network is profoundly affected by its internal architecture (the number hidden layers and the number of neurons in each one) and the type of interconnections (feed-forward, recursive, winner-take-all, etc.). The exact shape of the activation function has limited effects on the overall performance and is usually set according to the needs of the training heuristics (a sigmoid function in the case of back-propagation method). There is no general mathematical theory but rather a number of empirical rules to be considered when constructing such models. The architecture of the neural module adopted in this work is shown in Fig. (2). It is constituted of one feed forward module containing $N_1 \times N_2$ input neurons, a single hidden layers containing M neurons each and 5 output neurons. These parameters were set after an exploratory analysis aiming at optimizing the performance of the system, considering simultaneously the computational effort (which delays the output) and the probability of correct regime identification. Each neuron at the output layer is responsible for identifying one of the following five horizontal gas-liquid regimes: stratified smooth, stratified wavy, intermittent, bubbly and annular. The training procedure constitutes in acquiring pressure signals from known flow regimes (determined both visually and with the help of Taitel and Dukler´s map (Taitel and Dukler, 1976) and by setting the desired output values to zero, except for the neuron corresponding to the flow regime which is set to one. Several and varied example signals were taken from each flow regime to compose the training data set.

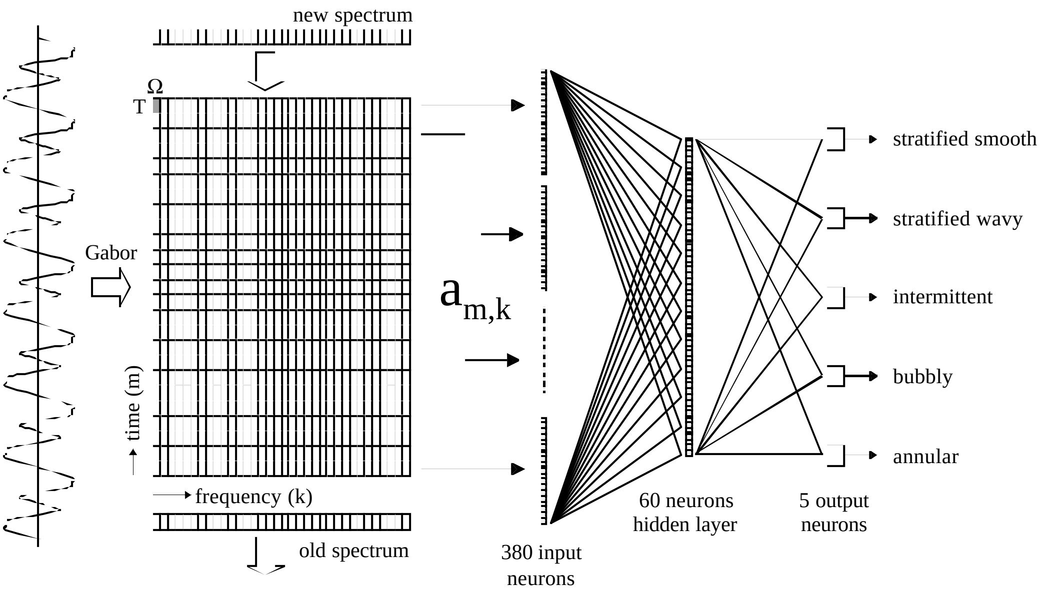

Figure 2. Neural network architecture adopted in this work (the inputs are the Gabor coefficients calculated with (12) and the outputs are numbers varying between 0 and 1 indicating, respectively, if a particular regime was not detected or positively detected)

4. Experimental circuit, instrumentation and software

Different horizontal air-water flow regimes were generated in an experimental loop at the Thermal and Fluids Engineering Laboratory of the University of São Paulo at São Carlos – Brazil. The test section is constructed in Plexiglas and has an internal diameter of 30 mm and a total length of 12 m. It is mounted on an articulated structure that can be inclined between $\pm 10^o$ approximately. Air is supplied by a 47 kW screw compressor. The flow rate is controlled through servo-valves (Smar FY-301) and orifice plates (ASME MFC-3M-1998) installed in parallel lines to allow independent operation. SMAR LD301 and Danfoss MBS33 pressure transducers are responsible for measuring the differential pressure and the upstream static pressure respectively. Water is supplied by a 10 kW pump which is controlled by a frequency converter (Yaskawa VFD-B). The flow rate is measured by an orifice plate. The loop was conceived to be able to work with a second liquid, oil for instance, which is pumped through a 20 kW pump also controlled by a frequency converter and an orifice plate. The three fluid lines are connected to a mixing device designed to create extremely unstable flow structures in order to minimize the stabilization length downstream. A primary separator, connected by a flexible tube to the test section, is responsible for the separation of the gas phase and by pre-separating the liquid phases. Secondary separators are responsible for the final separation of the liquids that are recirculated through the corresponding pumps. The following figure illustrates NETeF's experimental loop.

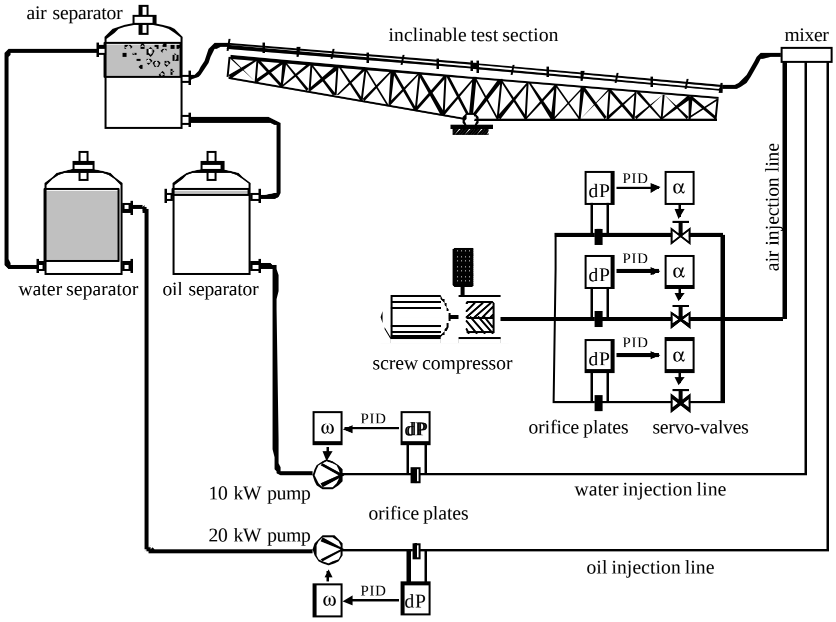

Figure 3. NETeF's experimental loop designed to reproduce the main flow regimes associated with gas-liquid and gas-liquid-liquid flows (the test section is inclinable by $\pm$ 10^{o} approximately)

A driver written in LabView© and implemented on a 500 MHz Pentium based computer is responsible for acquiring the signals from the pressure transducers and by controlling the servo-valves and the frequency converters through PID algorithms. The acquisition system is supplied by National Instruments and is constituted of an A/D AT-MIO-16DE10 board connected to a SCXI-1000 chassis with two SCXI-1331 multiplexers and SCXI-1180 feed through modules. The analog outputs of the acquisition system are connected to the servo-valves and to the frequency converters via Smar AM01P auto/manual transfer modules, which allow automatic control by the soft driver or direct manual control by the user. The following figure illustrates the acquisition system described above.

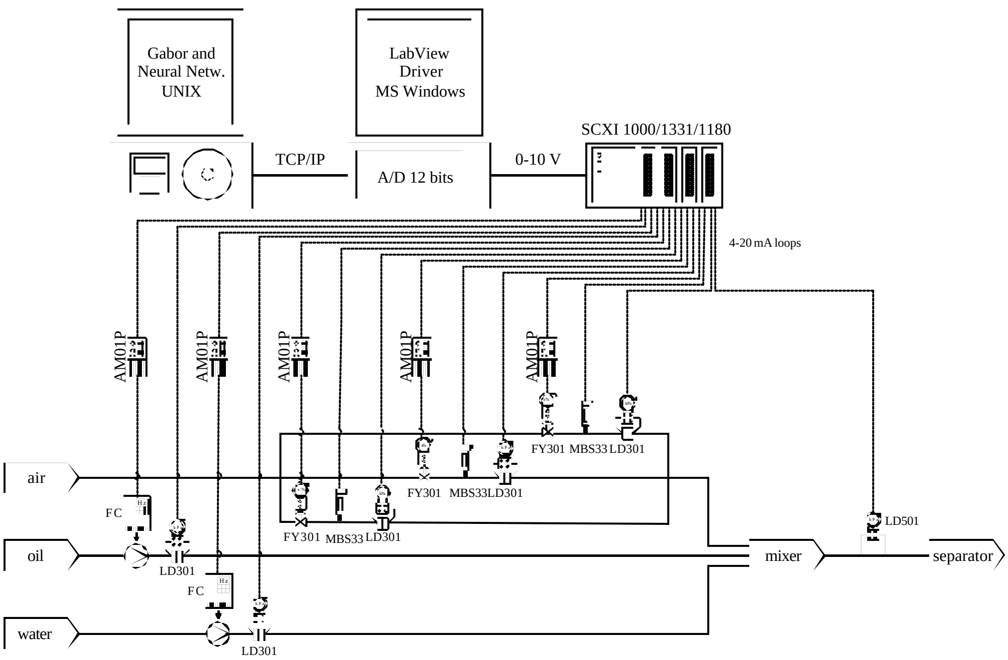

Figure 4. Schematic representation of the acquisition system and of the control instrumentation

The pressure transducer used for regime identification is a Smar LD501 model, with a cutoff frequency of approximately of 15 Hz. As indicated in Fig. (4) its connections were positioned 200 mm apart at the bottom of the test section in order to assess the longitudinal pressure gradient ($dP/dL \cong \Delta P/\Delta L$), also called fluctuating pressure. Some preliminary tests were made to determine the necessary pressure range to encompass all flow regimes. The transducer was then recalibrated in the range 0 – 100 mbar. The signal delivered by the LD501 transducer was acquired at 50 Hz to avoid aliasing effects and transferred via TCP/IP to a UNIX based machine to be processed separately from the loop's control routines. A UNIX machine was chosen because of its higher computational performance in on-line Gabor transforming the signal and processing the resulting coefficients through the neural network to determine the flow regime. The software for both calculations was developed in ANSI C. The neural network was trained using SNNS – Stutgart Neural Network Simulator (http://www-ra.informatik.uni-tuebingen.de/SNNS), and the converged weights and bias were exported to the on-line calculating neural module already mentioned.

5. Experimental tests and results

As previously stated, several fluctuating pressure signals were randomly sampled from each flow regime in order to constitute a representative training data set, particularly regarding the possible existence of unknown sub-regimes, which is very likely in intermittent flow (Klein et al., 2004). These signals were acquired at 50 Hz during at least 20.48 seconds which corresponds to a minimum of 1024 samples. Low velocity flows, characterized by a spectral content centered on 0.25 Hz, required longer acquisition periods of up to 16384 samples or 327.7 seconds. The following figure shows the area on Taitel and Dukler's map from which the signals were sampled, defined by the maximum flow rates supplied by the water pump and by the compressor. The lower limits, indicated by the dashed lines, are associated with the stability of the flow rates in steady state operation, what is related with the influence of the resolution of the flow metering instruments on the PID algorithms.

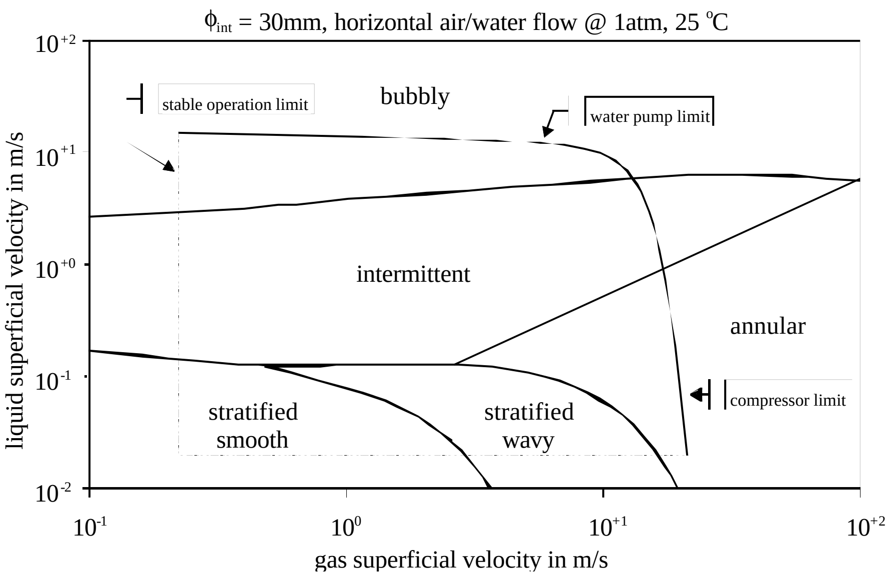

Figure 5. Region in Taitel and Dukler's map from which the training signals were randomly sampled

The intrinsic parameters in Gabor transforming the pressure signals were determined after an exploratory analysis in which the performance of the system was optimized, considering both computational efficiency and the percentage of correct regime identification. More specifically, an exact partition of the time-frequency plane was chosen ($\beta = 1$) with $T = 0.5$ s and $\Omega = 0.63$ rad/s (= 0.1 Hertz). The decaying speed of the Gaussian window was set to $\alpha = 0.01\,s^{-2}$, what results in 19 (N_1) and 20 (N_2) significant coefficients respectively in time and frequency directions. Thus, the total number of time-frequency coefficients given by equation (12) results in 380 (the number on input neurons in the neural model), or 19 instantaneous spectra with 20 frequency amplitudes each, as indicated in Fig. (2).

The performance of the proposed flow regime identification methodology can be assessed in several ways. Recalling that the desired target values are exclusively 1 or 0, and that the obtained output values ξ vary continuously between these limits, it is convenient to define the following errors:

$$\left.\begin{aligned} e_{smooth} &= \sqrt{(1-\xi_1)^2+(0-\xi_2)^2+(0-\xi_3)^2+(0-\xi_4)^2+(0-\xi_5)^2} \\ e_{wavy} &= \sqrt{(0-\xi_1)^2+(1-\xi_2)^2+(0-\xi_3)^2+(0-\xi_4)^2+(0-\xi_5)^2} \\ e_{interm} &= \sqrt{(0-\xi_1)^2+(0-\xi_2)^2+(1-\xi_3)^2+(0-\xi_4)^2+(0-\xi_5)^2} \\ e_{bubbly} &= \sqrt{(0-\xi_1)^2+(0-\xi_2)^2+(0-\xi_3)^2+(1-\xi_4)^2+(0-\xi_5)^2} \\ e_{annular} &= \sqrt{(0-\xi_1)^2+(0-\xi_2)^2+(0-\xi_3)^2+(0-\xi_4)^2+(1-\xi_5)^2} \end{aligned}\right\} \overset{?}{\leq} e_{limit} \qquad (17)$$

It is important to stress that these errors can be calculated on-line for each acquisition step and thus can be monitored with respect to threshold levels or identification limits (e_{limit}). In other words, a specific flow regime is identified if its corresponding error signal falls below a conveniently predefined value for e_{limit}. The certainty of the identification procedure can then be defined as the number of correct hits divided by the number of signal of that particular regime that were sampled from the network's training region in Taitel and Dukler's map. Obviously the higher is the identification limit the greater is the certainty and vice-versa, tending to zero when $e_{limit} = 0$. The results obtained in this work are shown in Tab. (1) from where it can be seen that 100% certainty is achieved for $e_{limit} = 0.050$, corresponding to an extremely good performance. It is also possible to notice that intermittent flow regimes were identified with greater certainty. This can be attributed to the very characteristic time-frequency signature of these flow regimes, dominated by the intermittency frequency. This is equally the case for stratified wavy flows, which also have a strong time-frequency signature marked by the oscillation frequency of the stratification interface, and which were identified with the second best certainties. The lowest certainties were obtained for annular flows, what can be probably explained by the fact that these flows were sampled too close to the transitions to intermittent and to stratified flows due to limitations in the maximum air flow rate supplied by the compressor.

Table 1. Certainty of the flow regime identification determined with respect to different identification levels in (17)

identification limit	**flow regimes ?**	**stratified smooth**	**stratified wavy**	**intermittent**	**bubbly**	**annular**
	number of signals ?	**320**	**875**	**2098**	**313**	**348**
0.0500	hits	320	875	2098	313	348
	mistakes	0	0	0	0	0
	certainty	**100 %**	**100 %**	**100 %**	**100 %**	**100 %**
0.0045	hits	294	822	2001	293	303
	mistakes	26	53	97	20	45
	certainty	**91.87 %**	**93.94 %**	**95.37 %**	**93.61 %**	**87.07 %**
0.0040	hits	289	805	1962	279	281
	mistakes	31	70	136	34	67
	certainty	**90.31 %**	**92.00 %**	**93.52 %**	**89.14 %**	**80.74 %**
0.0030	hits	271	758	1889	255	240
	mistakes	49	117	209	58	108
	certainty	**84.68 %**	**86.63 %**	**90.04 %**	**81.47 %**	**68.96 %**
0.0020	hits	251	703	1794	211	190
	mistakes	69	172	304	102	158
	certainty	**78.44 %**	**80.34 %**	**85.51 %**	**67.41 %**	**54.59 %**
0.0010	hits	205	570	1582	152	109
	mistakes	115	305	516	161	239
	certainty	**64.06 %**	**65.14 %**	**75.40 %**	**48.56 %**	**31.32 %**

6. Conclusions and perspectives

A procedure for the on-line identification of horizontal gas-liquid flow regimes was developed in this work. The procedure is based on acquiring pressure gradient signals (fluctuating pressure) and on its subsequent decomposition into time-frequency coefficients associated with the Gabor transform, followed by their analysis through a previously trained neural model. Experimental tests were performed to validate and to assess the performance of the proposed identification procedure. Different horizontal air-water flow regimes were generated in the experimental loop of the Thermal and Fluids Engineering Laboratory of the University of São Paulo at São Carlos – Brazil. The test section is 12 m long and has an internal diameter of 30 mm. The network's training procedure constituted in acquiring pressure signals from known flow regimes and by setting the desired output values to zero, except for the neuron corresponding to the flow regime which is set to one. A total number of 3954 example signals were sampled from all flow regimes to compose the training data set. This dataset also permitted to determine the performance of the proposed procedure, particularly in what regards the certainty associated with the identification of each flow regime. An overall certainty of 100% is achieved when the detection level is set to 0.050 in (17). Intermittent and stratified wavy regimes were identified with greater certainty, what can be attributed to its marked time-frequency signature, associated with the intermittency frequency and with the oscillation frequency of the stratification interface respectively. The lowest certainties were obtained for annular flows, probably because this regime was not properly explored due to limitations in the maximum air flow rate supplied by the compressor. Future work should include new experiments with different inclinations of the test section and also the detection of anomalies, such as a breach in the pipeline or instance. It would be equally interesting to study the influence of the density of the partition of the time-frequency plane, given by β in (11), and of the number of neurons in the hidden layer of the neural model on the global performance of the identification procedure.

7. Acknowledgement

The authors would like to acknowledge the financial support provided by FAPESP (grant 98/129221-1) and CNPq (grant 62.0012/99-4).

8. References

Bannwart, A. C., 2001, Modeling aspects of oil-water core-annular flows, Journal of Petroleum Science And Engineering , 32 (2-4): pp.127-143

Cohen, L., 1995, Time frequency analysis, Englewood Cliffs : Prentice Hall, 299p.

Crivelaro, K. C. O., Hervieu, E., Seleghim Jr., P., Identification of horizontal two-phase flow regimes through a neural network models. Journal of the Brazilian Society of Mechanical Sciences. , v.14, n.1, p.1 - 16, 2002

Drahos J. & Cermák J., 1989, "Diagnostics of gas-liquid flow patterns in chemical engineering systems", Chemical Engineering Processes, Vol. 26, pp. 147-164

Gabor D., 1946, Theory of Communication. J. IEE, Part III, London, pp. 429-457

Hervieu E, Seleghim P, 1998, An objective indicator for two-phase flow pattern transition, Nuclear Eng. Design, Vol. 184: (2-3), pp. 421-435

Hervieu E. & Leducq D., 1991, "The wavelet transform as a diagnostic tool in two-phase flows : characterisation of multiphase flows from wall measurements", European Two-Phase Flow Group Meeting, Rome

Hubbard M.G. & Dukler A.E., 1966, "The characterization of flow regimes for horizontal two-phase flow", Proc. Heat Transfer and Fluid Mech. Institute. Stanford University Press - M.A. Saad & J.A. Moller eds.

Klein F. L., Seleghim Jr. P. and Hervieu E., Time-Frequency Analysis of Intermittent Two-Phase Flows in Horizontal Piping. Journal of the Brazilian Society of Mechanical Sciences and Engineering, accepted for publication.

Klein, F. L., Seleghim, Jr. P. and Hervieu E., 2004, Time-frequency analysis of intermittent two-phase flows in horizontal piping, accepted for publication in Journal of the Brazilian Society of Mechanical Sciences.

Mi Y., M. Ishii, L. H. Tsoukalas, 1998, Vertical two-phase flow identification using advanced instrumentation and neural networks, Nuclear Engineering and Design Vol. 184 pp.409-420

Seleghim Jr. P., Hervieu, E. and Santos A. M., Time-Frequency Characterisation of Two-Phase Horizontal Air-Water Flow Regimes. Journal of the Brazilian Society of Mechanical Sciences. Brasil: , v.20, n.3, p.1 - 14, 1998.

Seleghim P. Jr & Hervieu E., 1994, "Caractérisation des changements de configuration des écoulements diphasiques gaz-liquide par analyse de la fréquence instantanée", C.R. Acad. Sci. Paris, t. 319, Série II, pp. 611-616

Taitel Y. & Dukler A.E., 1976, "A model for predicting flow regime transitions in horizontal and near horizontal gas-liquid flow", AIChE Journal, Vol. 22, N°1, pp. 47-55

Yan H., Liu Y. H. and Liu C. T., 2004, Identification of flow regimes using back-propagation networks trained on simulated data based on a capacitance tomography sensor, Measurement Science and Technolgy. Vol.15, pp. 432–436.